

Full-Scale Self-Emissive Blue and Green Microdisplays Based on GaN Micro-LED Arrays

J. Day¹, J. Li², D. Y. C. Lie¹, C. Bradford³, J. Y. Lin^{1a)}, and H. X. Jiang^{1a)}

¹ Department of Electrical and Computer Engineering, Texas Tech University, Lubbock, TX 79409

² III-N Technology, Inc, Lubbock, TX 79416

³ US Army, RDECOM CERDEC Night Vision and Electronic Sensors Directorate, 10221 Burbeck Road, Ft. Belvoir, VA 22060

ABSTRACT

Micro-size light emitting diode (μ LED) arrays based on III-nitride semiconductors have emerged as a promising technology for a wide range of applications. If InGaN μ LED arrays can be integrated on to Si complementary metal-oxide-semiconductor (CMOS) substrates for active driving, these devices could play crucial roles in ultra-portable products such as next generation pico-projectors, as well as in emerging fields such as biophotonics and optogenetics. Here we present a demonstration of, and methods for, creating a high-resolution solid-state self-emissive microdisplay based on InGaN/GaN semiconductors. An energy efficient active drive scheme is accomplished by integrating micro-emitter arrays with CMOS active matrix drivers that are flip-chip bonded together via indium metal bumps.

Keywords: Solid-state microdisplays, self-emissive displays, micro-LED array, III-nitride wide bandgap semiconductors, III-V and CMOS integration, active drive, flip-chip bonding

1. INTRODUCTION

In the last twenty years, high brightness LEDs based on III-nitride semiconductors have achieved dramatic advances alongside developments in indicators and solid-state lighting¹. For example, InGaN-based white emitters have achieved a luminous efficacy of more than 150 lm/W, which is much higher than those of other self-emissive devices, such as organic LEDs (OLEDs) and electroluminescent emitters¹. With the incorporation of multiple quantum wells (MQW) as the active region, LEDs have a narrow emission band of about 25 nm, providing a basis for high color purity and chromatic fidelity. With their intrinsic material properties and low voltage operation characteristics, LEDs have a much longer operational lifetime (> 100,000 hours), can be operated at extreme conditions such as high or low temperatures (-100° to 120° C) and humidity. All of these intrinsic properties make LEDs an ideal candidate for many applications where performance, reliability and lifetime are critical.

Since their inception³⁻⁷, μ LED arrays based on III-nitride semiconductors have emerged as a promising technology for applications, including self-emissive microdisplays⁵⁻⁸, single-chip high voltage AC-LEDs for solid-state lighting⁹⁻¹¹, and light sources for optogenetic neuromodulation¹²⁻¹⁵. The InGaN-based μ LED array has opened a new avenue for the multi-site photostimulation of neuron cells and offers the opportunity to probe biological neuron networks at the network level^{13,14}. In particular, III-nitride μ LED arrays provide high brightness/contrast/resolution/reliability, long-life, compactness, operation under harsh

conditions and under bright daylight – properties which cannot be matched by more conventional liquid crystal display (LCD), OLED, and digital light processing (DLP) based microdisplay technologies^{16,17}.

Here, we present a successful example of III-nitride μ LED array integration with Si CMOS to accomplish a high-resolution solid-state self-emissive microdisplay operating in an active driving scheme¹⁸. The fabricated blue or green video graphics array (VGA) microdisplays (640 x 480 pixels) have a pixel size of 12 μ m, a pitch distance of 15 μ m and are capable of delivering real time video graphics images. An energy efficient active driving scheme is accomplished by integrating micro-emitter arrays with CMOS active matrix drivers that are flip-chip bonded together via indium metal bumps. This success means that InGaN μ LED arrays could play crucial roles in emerging fields such as biophotonics and optogenetics¹²⁻¹⁵, as well as ultra-portable products such as next generation pico-projectors¹⁷.

There have been a few reports on monolithic III-nitride μ LED arrays⁵⁻⁸. A monolithic μ LED microdisplay is a microdisplay in which the μ LEDs themselves and the interconnection between these μ LEDs (the signal transmission paths, including all the metal lines for n- and p-type contacts) are all integrated on the same GaN wafer. This monolithic integration has the merits of easy and quick demonstration and characterization, since the microdisplay itself is an independent package, and the driving circuit can be designed using an off-the-shelf CMOS integrated circuit (IC) chip. However, to achieve a full-scale microdisplay in a monolithic μ LED array, connecting the huge amount of control signals from a separate driving circuit to the microdisplay within a limited space is a very difficult if not impossible task. For example, a monochrome VGA format microdisplay with 640 x 480 pixels requires a minimum of 1120 connections to the rows and columns in order to drive the microdisplay. Given a pixel pitch of 15 μ m (the perimeter of the microdisplay is only about 35 mm for VGA), wire bonding or tape bonding from the periphery matrix array pads to the driving circuit is highly challenging. A much more serious issue is the driving approach and the achievable performance¹⁶. Such a monolithic μ LED microdisplay connected with a separated driving circuit can only be driven in the passive mode. In this mode, one can only independently access one row at a time. Furthermore, the addressing time of each pixel, or the time one pixel is in the “on” state, is inversely proportional to the number of lines (rows) in the display matrix. The result is that under pulse driving, the brightness of the pixel is only $1/R$ (R defines the number of the rows) of the brightness under the equivalent DC current driving. In other words, to keep the same brightness, the driving current has to be increased by R times. For high-information-content (high-resolution) video displays, or for very high luminance-requirement sunlight readable displays, the maximum driving current limit is reached, and the light output saturates with further increase in current; hence the light efficiency and thermal dissipation become serious issues. For high-information-content displays, the desired driving approach is active matrix driving, which cannot easily be implemented in monolithic μ LED microdisplays. Until now, microdisplays based on inorganic semiconductors that are capable of delivering video graphics images have not been realized.

2. EXPERIMENT

In order to realize the full potentials of III-nitride μ LED arrays, developing schemes to actively and energy efficiently drive the devices is essential, since it is envisioned that these devices will be operated on battery power and the efficiency of all components in the device package directly affect how long it can operate between charging. The challenge for achieving such a device is that III-nitride micro-emitters cannot currently be fabricated directly over Si IC circuitry. To overcome the above difficulty, we have employed the hybrid μ LED microdisplay concept, similar to the widely deployed scheme of hybrid focal plane array detectors¹⁹, which utilizes the technique of flip-chip bonding via indium metal bumps. However, the typical size of indium metal bumps used in hybrid focal plane array detectors is around 20 μ m.

The μ LED layer structure used for microdisplay fabrication is shown in Fig. 1(a). Like conventional III-nitride LEDs, μ LED structures were grown on (0001) sapphire substrates by metal-organic chemical vapor deposition (MOCVD). The insulating sapphire substrate provides an ideal platform as the display surface and for isolation between individual μ LEDs. All of the emitter structures used are based on InGaN/GaN MQW confined between n-type and p-type GaN barriers. The emission wavelength was tuned by adjusting the In composition in InGaN alloys in the MQW active region. N- and p-GaN layers form the barriers and Ohmic contact layers. Effective hole injection is always an issue for III-nitride emitters due to

the relatively large activation energy of Mg acceptors and low conductivity of p-GaN²⁰. Reducing the contact resistance will enhance the hole injection efficiency, reduce threshold current and heat generation, and increase the device operating lifetime. For improved performance, we have adopted heavily Mg doped p-type GaN (p⁺-GaN) layer as the contact layer to minimize the contact resistance²¹. The fabrication steps of III-nitride μ LED arrays were built on previously reported procedures for etching and metallization^{22,3-11}. CMOS active matrix 640 x 480 and 160 x120 microdisplay controller ICs with μ LED current of 0.5 μ A to 10 μ A have been designed and fabricated in a CMOS process.

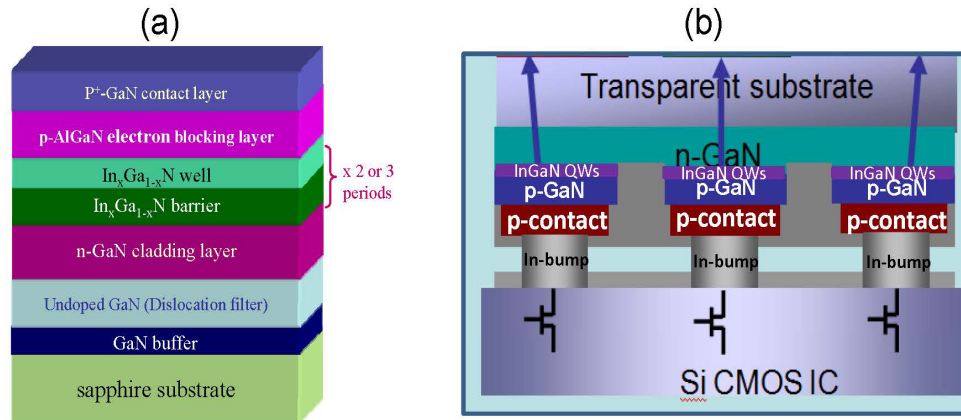


Fig. 1 (a) Layer structure of μ LED wafers. (b) Illustration of flip-chip bonding the μ LED matrix array with the CMOS IC driver chip via the indium bumps to form a highly integrated one package microdisplay.

Figure 1(b) shows schematic illustrations of the microdisplay which consists of an array of InGaIn micro-emitters as pixels arranged into matrix format on a sapphire substrate and the μ LED array is heterogeneously integrated on to a Si CMOS IC driver chip using indium bump bonding. The polished back surface of the transparent sapphire substrate is used to display images. The pixels share a common anode (n-type contact) with independently controllable cathode (p-type contact). The hybrid integration of the InGaIn microdisplay die with the Si CMOS driving circuit IC chip die means that hundreds or thousands of the signal connections between the microdisplay and the driving circuit have been accomplished in a single flip-chip bonding package through the indium metal bumps. This active matrix display also means that each pixel is geared with its own pixel driver circuit in CMOS that is capable of storing data and driving each individual μ LED. The interface requirements of this hybridized package are thereby reduced to the few lines required for the signal and power connections.

3. RESULTS AND DISCUSSIONS

An expanded view under an optical microscope of a segment of an individually diced μ LED array chip is shown in Fig. 2(a), which illustrates more details of the fabricated devices. Micro-LED pixels and indium metal bumps fabricated by thermal evaporation on the μ LED pixels seen from the transparent sapphire side are presented in Fig. 2(b). The results demonstrate $\sim 6 \mu\text{m}$ indium bumps with excellent size uniformity.

Figure 3(a) shows a fully assembled InGaIn microdisplay. Figure 3(b) shows a grayscale projected image of a leopard from a green InGaIn VGA microdisplay (having 640 x 480 pixels) and reveals that the fabricated microdisplays are capable of delivering real time video graphics images. Figure 4 shows the measured characteristics of InGaIn μ LED pixels for blue and green microdisplays. The room temperature optical power shown in Fig. 4 was measured by a calibrated optical power meter placed on the sapphire side of a μ LED array when a single pixel was lit. The nearly linear optical power output with increasing forward

current will be very useful for a range of applications, and ensures a high brightness microdisplay with a high dynamic range gray scale.

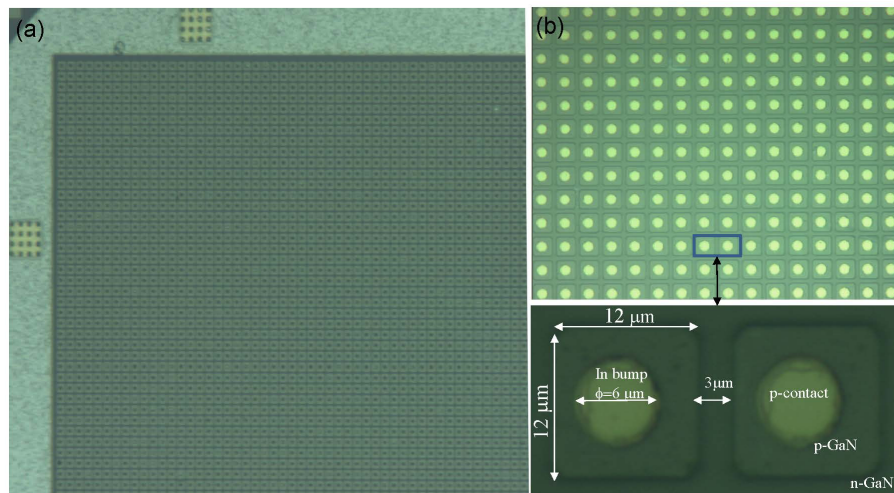


Fig. 2 Optical microscopy images of a full scale (640 x 480 pixels) InGaN μ LED array. (a) The zoom-in image of a segment of a full scale InGaN μ LED array chip. (b) The zoom-in image of a flip-chip bonded package with μ LED pixels and indium bumps viewed from the transparent sapphire side.

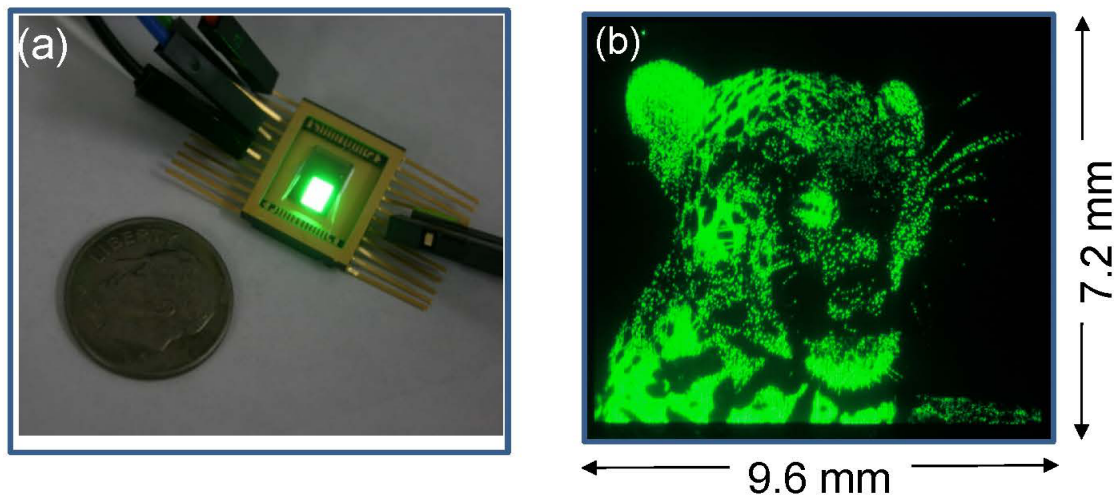


Fig. 3 Demonstration of an III-nitride self-emissive microdisplay. (a) A fully assembled InGaN microdisplay operating at a driving current of about $1 \mu\text{A}$ per pixel. (b) A grayscale projected image of a leopard from a green VGA InGaN microdisplay (having 640 x 480 pixel with a pixel size of $12 \mu\text{m}$ and a pitch distance of $15 \mu\text{m}$) operating at a driving current of $1 \mu\text{A}$ per pixel.

To obtain a sense of the microdisplay brightness, we characterized the luminance of the green μ LED pixels. As shown in Fig. 5(a), a $12 \mu\text{m}$ pixel outputs roughly $1 \text{ mcd}/\mu\text{A}$ and the luminance increases almost linearly with driving current (I) for $I < 100 \mu\text{A}$. For a microdisplay with a pitch distance of $15 \mu\text{m}$, when

every pixel within the array is lit up and operates at $1 \mu\text{A}$, the brightness of the microdisplay can be calculated to be $\sim 4 \times 10^6 \text{ cd/m}^2$. This luminance level is several orders of magnitude higher than those of LCD and OLEDs. Based on the pixel characteristics in Fig. 4, at $I = 1 \mu\text{A}$, a green μLED pixel has a voltage of around 2.6 V. This means that the power dissipation within the μLED array is only about 0.8 W for a full VGA (640×480 pixels) microdisplay if every pixel within the μLED array is lit up simultaneously. This estimate represents the upper limit of power dissipation since normally only a fraction ($\sim 25\%$) of pixels are lit up for graphical video image displays. Notice also that $1 \mu\text{A}$ driving current translates to a current density of about 0.7 A/cm^2 for a $12 \mu\text{m}$ pixel, which is about $1/30$ of the typical value (22 A/cm^2) in conventional indicator LEDs, which have an average chip size of $300 \mu\text{m} \times 300 \mu\text{m}$ and an expected operating lifetime exceeding 100,000 hours under normal operating conditions (i.e., $I = 20 \text{ mA}$). These estimates also imply that the lifetime of III-nitride μLED array should be as long as those of indicator LEDs.

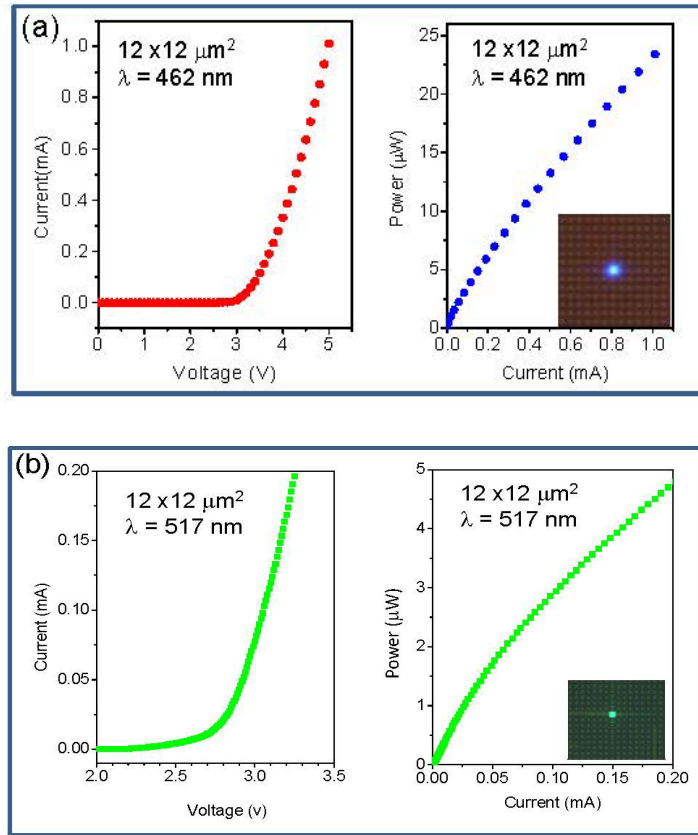


Fig. 4 Optoelectronic characteristics of μLED pixels. (a) I-V and L-I characteristics of blue μLED pixels. (b) I-V and L-I characteristics of green μLED pixels.

Another outstanding feature of InGaN based self-emissive microdisplays is their ability to operate under harsh conditions and at high or low temperatures. The operating temperature (T) dependence of the optical output power of our μLED s has been measured and the results are depicted in Fig. 5(b). For the temperature dependence and radiance characterization, passive μLED array chips with 16×16 pixels (with $12 \mu\text{m}$ pixel size and $15 \mu\text{m}$ pitch distance) were fabricated. The luminance of μLED was measured by using a bare green μLED array chip (16×16 pixels simultaneously on) in conjunction with a 10-inch integrating optical sphere, and the single pixel radiance shown in Fig. 5(a) was obtained by dividing the measured value by the number of pixels ($16 \times 16 = 256$). The temperature dependence of the relative optical power shown in Fig. 5(b) was measured by placing the optical power meter outside the optical window of a portable cryostat

while the μ LED array chip (16 x 16 pixels simultaneously on) was held inside the cryostat under a driving current of 0.1 mA. The intensity of the μ LED emission decreased by about 10% when T was raised from room temperature to +100 °C and remained almost constant when T was cooled down from room temperature to -100 °C, while the operating voltage at 0.1 mA varied from 4.1 V at -100 °C to 2.9 V at +100 °C. This continuous reduction in the operating voltage with increasing T is due to thermal activation of free holes (p) described by the process of $p \sim \exp(-E_A/kT)$, where the Mg acceptor activation energy (E_A) in GaN is about 160 meV. The T dependence of the μ LED emission intensity in Fig. 5(b) represents the lowest thermal quenching ever reported for any type of microdisplay. The outstanding thermal stability is a direct attribute of III-nitride semiconductors.

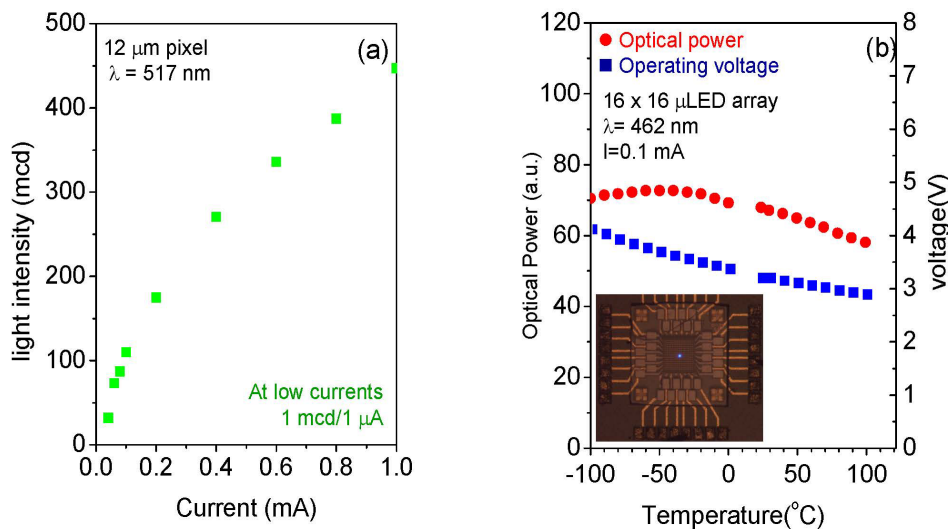


Fig. 5 Confirmation of exceptional brightness and high thermal stability of InGaN microdisplay. (a) Luminance of a green μ LED pixel as a function of driving current. (b) The temperature dependence of the relative emission optical power of an InGaN μ LED array.

4. SUMMARY

In summary, we have achieved prototype full scale (VGA) high-resolution (with 12 μ m pixel size and 15 μ m pitch) self-emissive blue/green microdisplays, which are capable of delivering video graphics images for high brightness pico-projector and head-up/wearable display applications. Key advances include: (1) low contact resistance of μ LEDs with 12 μ m pixel size; (2) design and fabrication of an active matrix microdisplay driver circuit implemented in a digital CMOS process; (3) successful hybrid integration of InGaN μ LED array die with Si CMOS IC chip die using flip-chip bonding via. Unique features of III-nitride microdisplays over other technologies are summarized in Table 1. Compared with microdisplays based on LCD, OLED, and DLP, microdisplays fabricated from III-nitride μ LED arrays can potentially provide superior performance. Unlike LCDs that normally require an external light source, III-nitride blue microdisplays are self-emissive and result in both space and power saving and allow viewing from any angle without color shift and degradation in contrast. On the other hand, OLEDs must be driven at current densities many orders of magnitude lower than semiconductor LEDs to obtain devices with a reasonable lifetime and hence are not suitable for high-intensity use. DLP and laser beam steering (LBS) devices require the use of rapidly scanning microelectromechanical (MEMS) mirrors and separate light sources such as LEDs or laser diodes (LDs), which adds complexity, volume, and cost to the devices. Furthermore, the service lifetimes of MEMS and LDs are shorter than LEDs. Another distinctive feature of III-nitride microdisplay is its operating speed. Based on time-resolved electro-luminescence measurement, III-nitride

μ LEDs have a very fast response⁴. The measured turn-on time is on the order of tens of picoseconds. The operating speed of a μ LED is limited by its turn-off time, which is on the order of 0.2 ns. This property ensures that the nitride μ LED based microdisplays have a much faster response than LCD and OLED based microdisplays and opens up their potential uses as light sources for site selective fluorescence lifetime studies.

Table 1 Comparison among various technologies for microdisplays.

Technology	Liquid Crystal	Organic LED	III-nitride μ LED	Digital light processing	Laser beam steering
Mechanism	Backlighting/LED	Self-emissive	Self-emissive	Backlighting/LED	Backlighting/LD
Luminous efficacy	Medium	Low	High	High	High
Luminance	3000 cd/m ² (full color) ~ 10 ⁴ cd/m ² (green)	1500 cd/m ² (full color) ~ 10 ³ cd/m ² (yellow)	~ 10 ⁵ cd/m ² (full color) ~ 10 ⁷ cd/m ² (blue/green)	~ 1000 cd/m ² (full color)	~ 1000 cd/m ² (full color)
Contrast ratio	200: 1 (intrinsic)	Very high > 10,000:1	Very high > 10,000:1	High	High
Response time	ms	μ s	ns	ms	ms
Operating temperature	0 to 60 °C Requires heater	-50 to 70 °C	-100 to 120 °C	To be determined	To be determined
Shock Resistance	Low	Medium	High	Medium	Medium
Lifetime	Medium	Medium	Long	Medium [limited by MEMS]	Short [limited by laser diodes]
Cost	Low	Low	Low	High	High

ACKNOWLEDGEMENT

This work is supported by ARMY contract # W909MY-09-C-0014. We thank Sixuan Jin and Weiping Zhao for their skillful help with lithography and device processing. We gratefully acknowledge useful discussions with Dr. Zhaoyang Fan of Texas Tech University and Dr. Russell Draper of US Army, Night Vision and Electronic Sensors Directorate. Lin and Jiang are also grateful to the AT&T Foundation for the support of Ed Whitacre and Linda Whitacre Endowed chairs.

REFERENCES

- a) hx.jiang@ttu.edu; jingyu.lin@ttu.edu
1. A. Bergh, G. Craford, A. Duggal, and R. Haitz, *Physics Today*, **54**, 42 (2001).
 2. Y. Narukawa, M. Sano, M. Ichikawa, S. Minato, T. Sakamoto, T. Yamada, and T. Mukai, *Jpn. J. Appl. Phys.* **46** L963 (2007).
 3. S. X. Jin, J. Li, J. Z. Li, J. Y. Lin, and H. X. Jiang, *Appl. Phys. Lett.* **76** 631 (1999).
 4. S. X. Jin, J. Li, J. Shakya, J. Y. Lin, and H. X. Jiang, *Appl. Phys. Lett.* **78** 3532 (2001).
 5. H. X. Jiang, S. X. Jin, J. Li, J. Shakya, and J. Y. Lin, *Appl. Phys. Lett.* **78** 1303 (2001).
 6. H. X. Jiang, S. X. Jin, J. Li, and J. Y. Lin, *US patent* 6410940 (2002).
 7. H. X. Jiang and J. Y. Lin, III-Nitride Quantum Devices – Microphotonics, *CRC Critical Reviews in Solid State and Materials Sciences*, (P. Holloway, Editor), **28**, 131 (2003).
 8. J. J. D. McKendry, B. R. Rae, Z. Gong, K. R., Muir, B. Guilhabert, D. Massoubre, E. Gu, D. Renshaw, M. D. Dawson, and R. K. Henderson, *IEEE photonics Technology Letters*, **21**, 811 (2009).
 9. H. X. Jiang, J. Y. Lin, and S. X. Jin, *US Patent* 6957899 (2005) and 7221044 (2007).
 10. Z. Y. Fan, J. Li, J. Y. Lin, and H. X. Jiang, *US Patent* 7714348 (2010).
 11. Z. Y. Fan, H. X. Jiang, and J. Y. Lin, *Journal of Physics D: Applied Physics*, **41**, 094001-094012 (2008).
 12. V. Poher, N. Grossman, G. T. Kennedy, K. Nikolic, H. X. Zhang, Z. Gong, E. M. Drakakis, E. Gu, M. D. Dawson, P.M.W. French, P. Degenaar, and M. A. Neil, *J. Phys. D: Appl. Phys.* **41**, 094014 (2008).
 13. N. Grossman, V. Poher, M. S. Grubb, G. T. Kennedy, K. Nikolic, B. McGovern, P. R. Berlinguer, Z. Gong, E. M. Drakakis, M. A. Neil, M. D. Dawson, J. Burrone, and P. Degenaar, *J. Neural Eng.* **7**, 016004 (2010).
 14. P. Degenaar, N. Grossman, M. Memon, J. Burrone, M. D. Dawson, E. Drakakis, M. A. Neil, K. Nikolic, *J. Neural Eng.* **6**, 035007 (2009).
 15. T. Young and C. Chen, *Biomaterials*, **27**, 3361 (2006).
 16. W. E. Howard and O. F. Prache, *IBM J. RES. & DEV.* **45**, 115 (2001).
 17. D. Vettese, *Nature Photonics* **4**, 752 (2010).
 18. J. Day, J. Li, D.Y.C. Lie, C. Bradford, J. Y. Lin, and H. X. Jiang, *Appl. Phys. Lett.* **99**, 031116(2011).
 19. P. Lamarre, A. Hairston, S. Tobin, K. K. Wong, M. F. Taylor, A. K. Sood, M. B. Reine, M. J.J. Schurman, I. T. Ferguson, R. Singh, and C. R. Eddy, Jr., *Mat. Res. Soc. Symp.* **639**, G10.9.1-G10.9.6 (2001).
 20. S. Nakamura, S. J. Pearton, and G. Fasol, G. The Blue Laser Diode. The Complete Story, *Meas. Sci. Technol.* **12** 755 (2001).
 21. J. Dennemarck, T. Böttcher, S. Figge, S. Einfeldt, R. Kröger, D. Hommel, E. Kaminska, W. Wiatroszak, and A. Piotrowska, *phys. stat. sol. (c)* **1**, 2537 (2004).
 22. S. J. Pearton, J. C. Zolper, R. J. Shul, and F. Ren, *J. Appl. Phys.* **86**, 1 (1999).